Full quadrature regeneration of QPSK signals using sequential phase sensitive amplification and parametric saturation

K. R. H. Bottrill,* G. Hesketh, L. Jones, F. Parmigiani, D.J. Richardson and P. Petropoulos

Optoelectronics Research Centre, University of Southampton, Southampton, SO17 1BJ, UK
**krhb1g12@soton.ac.uk*

Abstract: We demonstrate all-optical regeneration of both the phase and the amplitude of a 10 GBaud quadrature phase shift keying (QPSK) signal using two nonlinear stages. First we regenerate the phase using a wavelength converting phase sensitive amplifier and then we regenerate the amplitude using a saturated single-pump parametric amplifier, returning the signal to its original wavelength at the same time. We exploit the conjugating nature of the two processing stages to eliminate the intrinsic SPM distortion of the system, further improving performance.

OCIS codes: (200.6015) Signal regeneration; (190.4380) Nonlinear optics, four-wave mixing; (060.1155) All-optical networks.

References and links

1. P. V. Mamyshev, "All-optical data regeneration based on self-phase modulation effect," in *Proceedings of 24th European Conference on Optical Communication* (IEEE, 1998), vol. 1, pp. 475–476.
2. T. I. Lakoba and M. Vasilyev, "On multi-channel operation of phase-preserving 2R amplitude regenerator," Opt. Commun. **322**, 114 – 117 (2014).
3. T. Akiyama, M. Sugawara, and Y. Arakawa, "Quantum-dot semiconductor optical amplifiers," Proc. IEEE **95**, 1757–1766 (2007).
4. J. K. Lucek and K. Smith, "All-optical signal regenerator," Opt. Lett. **18**, 1226–1228 (1993).
5. K. Croussore, I. Kim, Y. Han, C. Kim, G. Li, and S. Radic, "Demonstration of phase-regeneration of DPSK signals based on phase-sensitive amplification," Opt. Express **13**, 3945–3950 (2005).
6. J. Kakande, R. Slavík, F. Parmigiani, A. Bogris, D. Syvridis, L. Grüner-Nielsen, R. Phelan, P. Petropoulos, and D. J. Richardson, "Multilevel quantization of optical phase in a novel coherent parametric mixer architecture," Nat. Photonics **5**, 748–752 (2011).
7. R. Slavík, F. Parmigiani, J. Kakande, C. Lundström, M. Sjödin, P. A. Andrekson, R. Weerasuriya, S. Sygletos, A. D. Ellis, L. Grüner-Nielsen, D. Jakobsen, S. Herstrøm, R. Phelan, J. O'Gorman, A. Bogris, D. Syvridis, S. Dasgupta, P. Petropoulos, and D. J. Richardson, "All-optical phase and amplitude regenerator for next-generation telecommunications systems," Nat. Photonics **4**, 690–695 (2010).
8. A. Striegler, M. Meissner, K. Cvecek, K. Sponsel, G. Leuchs, and B. Schmauss, "NOLM-based RZ-DPSK signal regeneration," IEEE Photon. Technol. Lett. **17**, 639–641 (2005).
9. C. Lundström, B. Corcoran, M. Karlsson, and P. A. Andrekson, "Phase and amplitude characteristics of a phase-sensitive amplifier operating in gain saturation," Opt. Express **20**, 21400–21412 (2012).
10. A. Mohajerin-Ariaei, Y. Akasaka, J. Y. Yang, M. R. Chitgarha, M. Ziyadi, Y. Cao, A. Almaiman, J. D. Touch, M. Tur, M. Sekiya, S. Takasaka, R. Sugizaki, C. Langrock, M. M. Fejer, and A. E. Willner, "Bit-rate-tunable regeneration of 30-Gbaud QPSK data using phase quantization and amplitude saturation," in *Proceedings of The European Conference on Optical Communication* (IEEE, 2014), pp. 1–3.
11. K. R. H. Bottrill, F. Parmigiani, D. J. Richardson, and P. Petropoulos, "Optical predistortion enabling phase preservation in optical signal processing demonstrated in fwm-based amplitude limiter," J. Lightw. Technol. **In Press**, 1–1 (2016).
12. K. R. Bottrill, L. Jones, F. Parmigiani, D. J. Richardson, and P. Petropoulos, "FWM-based, idler-free phase quantiser with flexible operating power," in *Optical Fiber Communication Conference* (Optical Society of America, 2015), p. W4C.3.
13. K. Bottrill, R. Kakarla, F. Parmigiani, D. Venkitesh, and P. Petropoulos, "Phase regeneration of QPSK signal in SOA using single-stage, wavelength converting PSA," IEEE Photon. Technol. Lett. **28**, 205–108 (2015).
14. K. R. H. Bottrill, F. Parmigiani, L. Jones, G. Hesketh, D. J. Richardson, and P. Petropoulos, "Phase and amplitude regeneration through sequential PSA and FWM saturation in HNLF," in *Proceedings of the European Conference on Optical Communication* (IEEE, 2015), p. We.3.6.3.

15. J. Kakande, R. Slavik, F. Parmigiani, P. Petropoulos, and D. Richardson, "All-optical processing of multi-level phase shift keyed signals," in *Optical Fiber Communication Conference* (Optical Society of America, 2012), p. OW1I.3.
16. K. R. H. Bottrill, G. Hesketh, F. Parmigiani, D. J. Richardson, and P. Petropoulos, "Optimisation of amplitude limiters for phase preservation based on the exact solution to degenerate four-wave mixing," Opt. Express **24**, 2774–2787 (2016).
17. G. Hesketh, K. R. H. Bottrill, F. Parmigiani, D. J. Richardson, and P. Petropoulos, "On the role of signal-pump ratio in FWM-based phase preserving amplitude regeneration," in *International Conference on Optical Networks ICTON '15*.

1. Introduction

A number of schemes to achieve all-optical signal regeneration have been reported over the years, with notable examples including Mamyshev regenerators [1, 2], various configurations of semiconductor optical amplifiers [3], and nonlinear optical loop mirrors [4], which were originally targeted at regenerating the amplitude of the then ubiquitous on-off keying format without the use of high-speed electronics. With the advent of coherent receivers, attention in the field of all-optical regeneration has more recently turned towards developing methods compatible with complex modulation formats, leading to a resurgence in research upon optical phase sensitive amplifiers (PSAs) capable of regenerating a signal's phase [5–7]. However, to provide a truly complete regenerative solution for complex formats, not only must the phase of a signal be regenerated, but so too must its amplitude. This is especially important when using PSAs for phase regeneration, as in many examples, the reduction of phase noise is associated with an undesireable increase in amplitude noise [6]. Some schemes opt to provide this complete solution by performing phase and amplitude regeneration simultaneously in one medium. This approach has been demonstrated using nonlinear optical loop mirrors (NOLMs) [8] and saturated PSAs [9], however, such techniques may compromise regenerative performance, with each underlying process bringing its own disparate requirements for optimisation and not always being scalable to higher order modulation formats.

The natural alternative is to simply perform amplitude and phase regeneration separately in two sequential stages [10], and although such an approach may increase system size, it also allows for the two underlying regenerative stages to be optimised for their task alone without compromise. We have recently shown [11] that phase preserving amplitude regeneration can be achieved in a saturated FWM-based amplitude regenerator by optically predistorting the signal with SPM during an initial FWM stage, and conjugating the signal during a second, amplitude squeezing stage. The first stage in that demonstration was chosen to be a simple, degenerate-pump wavelength converter, although it was discussed that this first stage could be replaced by any scheme capable of imparting SPM upon the signal. In the present demonstration, we do exactly this, and replace the first stage with a wavelength converting PSA-based, 4-level phase regenerator [12, 13]. This results in a system which uses only two nonlinear stages to achieve both phase and amplitude regeneration and highlights the benefits of exploiting conjugation between stages to compensate their intrinsic SPM. This effect allows a higher output optical signal to noise ratio (OSNR) to be extracted from the system, simply by increasing input signal launch powers to levels which would otherwise be forbidden due to concerns of accruing excessive SPM. This is particularly significant, as it means that additional benefits may be realised from combining regenerative systems, and that designing systems in isolation may not actually be the best indicator of their combined performance. This work expands upon that presented at ECOC 2015 [14], providing further elaboration of the concept, detailed discussion of the means of optimising the system and a thorough presentation of the performance of the system using signal noise statistics. We demonstrate the scheme upon a 10 GBaud QPSK signal, which we contaminate with varying levels of broadband phase noise, in addition to white noise from amplified spontaneous emission.

2. Concept

As previously mentioned, the present demonstration can be considered to be an instance of the two stage amplitude regenerator demonstrated in [11], with the first, wavelength converting stage replaced by the idler-free, wavelength converting phase regenerator demonstrated in [12, 13]. Hence, the complete system can be described by its two underlying subsystems: a wavelength converting idler-free PSA (upper yellow section of Fig. 1), used to achieve phase regeneration, and a saturated four-wave mixing (FWM) based wavelength converter (lower blue section of Fig. 1), used to achieve amplitude regeneration, which follows it.

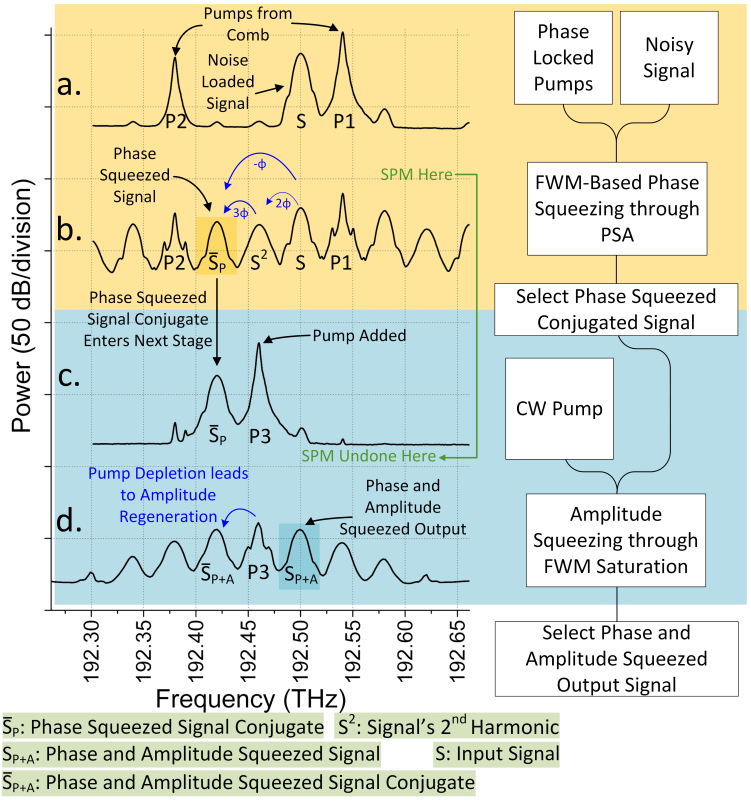

Fig. 1. Left: Spectra (a) Before PSA; (b) After PSA; (c) Before amplitude regeneration; (d) After amplitude regeneration. Right: Process resulting in corresponding spectra.

2.1. *Phase regenerator*

Phase squeezing of a QPSK signal, an example of an M-PSK signal with $M = 4$, can be achieved optically by coherently adding to it its conjugated $M - 1 = 3$rd harmonic [15]. The wavelength converting idler-free scheme used herein works analogously, but instead functions by coherently adding the conjugate of the signal to its unconjugated 3rd harmonic [12, 13].

Figure 1(a) shows the input of the nonlinear medium used to perform phase regeneration upon the signal. The signal, S is multiplexed with two phase locked CW pumps, P1 and P2. Figure 1(b) shows the result of allowing the input (Fig. 1(a)) to undergo FWM in the nonlinear medium. Two underlying FWM processes may be identified. One process, relying upon the interaction between P1 and S, produces a continuum of harmonics, with only the 3rd harmonic being of relevance to the functioning of the scheme. Meanwhile, a non-degenerate process between P1, P2 and S

results in the production of photons conjugated relative to the original signal. Due to the location of P2 (which is intentionally chosen to lie at the same wavelength as the 4th harmonic of the signal), the conjugated signal and the 3rd harmonic photons are added coherently.

As there is only one process which relies upon P2, the generation of conjugated signal photons, by controlling the power with which it enters the nonlinear medium, we may easily control the mixing factor, m, and hence the amount by which the phase of the signal is squeezed (in fact, m may be controlled by varying *any* of P1, P2 or S [12, 13]). By using a mixing factor of $m = 1/3$, we can achieve a flat-topped phase transfer profile [15].

2.2. Amplitude regenerator

Saturated FWM is ideal in this instance as not only does it perform amplitude squeezing, but it also offers the possibility of simultaneously compensating for the three other undesirable effects to which the signal was exposed during phase regeneration: wavelength conversion, conjugation and SPM. A side benefit of this approach is that implementation is relatively simple; procedurally, all that is required is to multiplex a pump with the signal and allow them to mix, tuning their launch powers such that the gain the signal experiences saturates [16]. Figure 1(c) shows the phase regenerated signal, $\bar{\mathrm{S}}_P$, coupled with the pump, P3, before it is launched into the fibre, whilst Fig. 1(d) shows the continuum of harmonics that results from allowing them to undergo FWM.

In [16], two sources of amplitude noise to phase noise conversion during degenerate FWM were identified, SPM and Bessel-order mixing (BOM) and it was shown that both can be reduced by increasing the pump to signal power ratio used to achieve saturation. In [11], the need to increase pump power was circumvented by predistorting the signal in a first nonlinear stage before performing saturation. By carefully tuning the signal launch powers in the two nonlinear media, the SPM and BOM between the two nonlinear stages can be balanced such that they largely negate each other, resulting in phase preserving operation. This is the exact principle exploited here to mitigate the SPM and BOM which are intrinsically present in both stages of phase and amplitude regeneration. It should be noted that BOM cannot be entirely negated between nonlinear stages, however, by careful tuning of the signal launch power in each FWM stage, residual BOM can be drastically reduced using the SPM of the second stage [11]. We apply this principle to the present case, noting that, although the action of the PSA combined with its intrinsic SPM may result in amplitude to phase noise characteristics not entirely identical to those of pure SPM, we may nonetheless compensate for them to some extent using the SPM of the second stage.

Cross-phase modulation (XPM) provides a mechanism for the conversion of the amplitude noise of the pumps into phase noise of the signal and its idlers. Provided the amplitude noise of the pumps is sufficiently low and the pump to signal ratio is not excessively high, XPM will not constitute a notable source of phase noise compared to the other noise processes involved [16, 17], instead being predominantly responsible for a constant and hence inconsequential phase rotation of the entire signal. The conditions used in the present study are practically the same as those used in [16], wherein it was shown that XPM indeed has a negligible impact on the phase noise of the system, and so we will not consider its action throughout the present discussion.

3. Experimental setup

We combine the two subsystems above, one after the other, resulting in the experimental setup shown in Fig. 2, with its various subsystems identified by coloured boxes, [14]. Firstly, a CW laser operating at 192.5 THz is divided into two paths with a fibre coupler. Using an IQ modulator, one path is modulated with a 10 GBaud non-return-to-zero QPSK signal, carrying two quadrature multiplexed PRBS-15 data streams.

This signal then passes into the noise loading stage which facilitates the contamination of the signal with a controllable amount of phase noise and in-band white noise. Phase noise is applied

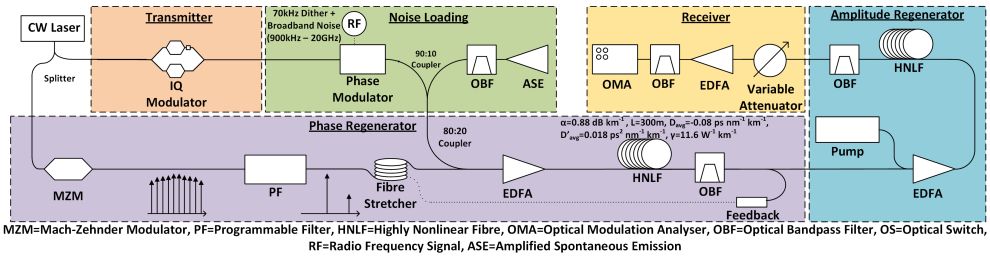

Fig. 2. Experimental setup of the regenerator showing the two underlying phase and amplitude regenerative stages.

by passing the signal through a phase modulator which is driven by broadband electrical noise, which is itself obtained by detecting amplified spontaneous emission (ASE) from an unseeded EDFA using a photodetector and then amplified to drive the modulator. A small sinusoidal dither of frequency 70 kHz is electrically diplexed with the noise signal before it drives the phase modulator, to facilitate phase tracking after PSA. *In-band* white noise is added to the signal by coupling into the signal path, ASE which has been filtered to the same bandwidth as the signal using an optical bandpass filter.

Meanwhile, the other path of the CW laser is modulated using a Mach-Zehnder modulator to produce an optical frequency comb with a 40 GHz frequency spacing. This optical frequency comb then passes through a programmable filter, which allows for the comb lines which are to be used as pumps for the PSA to be selected out. Sourcing the pumps from an optical frequency comb seeded by the same carrier as the signal simplifies achieving phase locking between the pumps and the signal, a requirement for the PSA to function correctly. Upon leaving the programmable filter, the two pump lines pass through a fibre stretcher which is driven by a feedback loop, discussed later.

The pumps and noise loaded signal are then combined before being amplified using an EDFA, after which they are launched into a 300 m spool of linearly strained HNLF (with nonlinear coefficient, γ =11.6 $\mathrm{W^{-1}km^{-1}}$ and Brillouin threshold P_{th} =24 dBm) to undergo FWM in the PSA stage. The phase squeezed signal is then filtered out using an optical bandpass filter located at 192.42 THz. A small amount of this signal is tapped off using a coupler and detected by a photodetector. Due to phase to amplitude conversion in the PSA, the 70 kHz phase dither added to the signal in the noise loading stage has now been converted to an amplitude dither, and is hence now detectable in the output of the photodetector. A lock-in amplifier is used to detect the amplitude of the 70 kHz dither in the optical signal and is passed to a proportional-integral-derivative controller (PID) to be used as an error signal. The set-point of the PID is chosen to minimise the magnitude of the 70 kHz dither and the output of the PID used to drive the fibre stretcher, forming a feedback loop and essentially enabling the carrier phase of the signal to be tracked.

After the signal's phase has been squeezed by the PSA, the signal enters the amplitude regenerator stage. All that is required is for a CW pump located at a frequency of 192.46 THz to be added to the signal and the signal and pump pair amplified before entering a 2 km cascade of HNLFs (two types of fibre were used: a total of 0.283 km of aluminium doped dispersion flattened HNLF followed by a total of 1.7 km of germanium doped dispersion flattened HNLF, which had attenuations of about 15 $\mathrm{dBkm^{-1}}$ and 1 $\mathrm{dBkm^{-1}}$, respectively and nonlinear coefficients of about 7 $\mathrm{W^{-1}km^{-1}}$ and 11.6 $\mathrm{W^{-1}km^{-1}}$, respectivey) to undergo amplitude saturation, with individual fibre segments connected by optical isolators to increase the Brillouin threshold of the cascade. After the HNLF, the amplitude squeezed signal is filtered out using an optical bandpass filter centred at 192.5 THz, the frequency of the original signal, after which it is launched into the

receiver.

In the receiver, before detection, the signal is loaded with a controllable amount of ASE (to facilitate measurements of receiver sensitivity), filtered and then analysed using an optical modulation analyser (OMA).

4. Results

For a given total power launched into the first stage, it was first determined how best to distribute the power between P1, P2 and S in order to maximise system performance. Figure 3 shows the result of operating the phase regenerating stage using mutually coherent, in phase (to provoke maximum phase sensitive gain) CW lines and a fixed total power launched into the nonlinear medium. Measurements of the output signal OSNR (identified in Fig. 3(a)) were taken for a range of P1:S power ratios, with the power of P2 tuned each time to achieve the same mixing factor, $m = 0.33$. Measurements were performed for three different total powers launched into the nonlinear medium, 21.5 dBm, 23.5 dBm and 25.5 dBm, with the results plotted in Fig. 3(b). The first point to notice is that output OSNR increases with increasing total launch power, as might be expected. If we now consider the results for each pump power separately, it can be seen that each curve roughly traces a parabola, with maxima obtained for a P1 : S ratio of approximately 2.5 dB. The shape of the curves arises from the complex interplay between the various FWM processes taking place, and it is easy to see that, in terms of SPM and OSNR, there is no benefit to be had from increasing P1 : S beyond 2.5 dB. However, for P1 : S $<$ 2.5 dB, a trade-off can be seen between OSNR and SPM; increasing one by increasing the signal power will necessarily increase the other. In the present case, however, as any SPM accrued in the first stage may be undone by the second, we were free to ignore the accrual of SPM in the first stage and optimise the first stage to maximise OSNR above all else. Hence, we chose to operate the phase regenerator with P1 : S =2.5 dB, which resulted in a peak in output OSNR of the system when a pump power of 22.5 dBm was used (the pump power chosen to ensure the system would not suffer due to stimulated Brillouin scattering). With these parameters determined, optimisation consisted of searching for a value of P3 : $\bar{\mathrm{S}}_{P+A}$ which minimised output phase noise (indicating that SPM compensation is optimal) when the system was saturated by increasing P3 + $\bar{\mathrm{S}}_{P+A}$ (with the system assumed to be saturated when output amplitude noise was minimised). Using the outlined process of optimisation, it was found that, when operating the PSA with the above parameters, the amplitude limiter should be operated with P3 =34 dBm and S =18 dBm.

After optimisation, the performance of the regenerator was first characterised in terms of its signal noise statistics at various stages of the system. Using the noise loading stage shown in Fig. 2, three statistical measures of the QPSK signal were mapped, phase noise ($\Delta\phi$), magnitude noise (ΔMag) and error vector magnitude (EVM), as they vary with input noise. Figure 4 contains the results of this measurement performed at three different points in the system: before regeneration (open circles), just after the PSA (crossed circles) and after both the PSA and amplitude limiter (solid circles). The left column (a-c) of Fig. 4 shows how the output statistics vary as the signal is loaded with phase noise whilst holding the amplitude noise fixed, whilst the middle column (d-f) shows the output statistics when we contaminate the signal with ASE only and the right hand column (g-i) provides output statistics where a fixed high level of ASE is added to the system with additional phase noise being varied.

Focusing first upon Fig. 4(a) we see that the system results in a decrease of $\Delta\phi_{out}$ for values of $\Delta\phi_{in} > 4$ deg. rms. Performing amplitude regeneration after phase regeneration has very little effect on $\Delta\phi_{out}$ due to the low $\Delta\mathrm{Mag}_{in}$ of the input signal and hence also limited SPM.

After passing through the PSA, there is a notable increase in $\Delta\mathrm{Mag}_{out}$ (Fig. 4(b)), increasing with additional phase noise which results from the phase dependent gain of the regenerator. For the highest input phase noise tested of $\Delta\phi_{in}$ =12.4 deg rms, magnitude noise can be seen to double from 5.6 %rms before regeneration to 10.9 %rms after PSA. After amplitude regeneration,

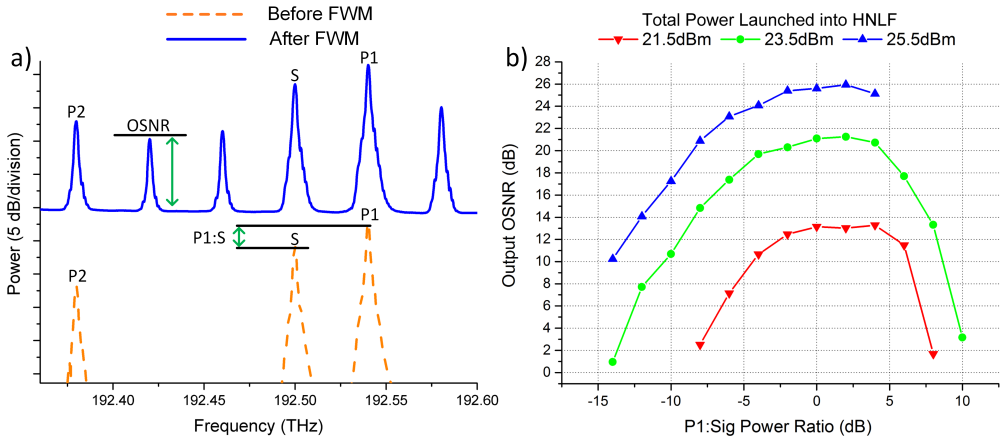

Fig. 3. (a) Spectrum identifying the pump to signal power ratio, P1 : S. (b) Plot of output OSNR of regenerated signal against P1 : S for three different total launch powers into the fibre.

the amplitude noise is reduced to 6.3 %rms, which is comparable to the input magnitude noise. As mentioned above, the middle column of Fig. 4 corresponds to the scenario whereby white noise in the form of ASE was added to the signal whilst otherwise adding no additional phase noise to the signal. The phase noise statistics in Fig. 4(d) show that phase regeneration is of benefit for values of EVM beyond 11% rms, which corresponds to a phase noise of about $\Delta\phi_{in} = 4.5$ deg. rms, comparable with the results in the phase noise loading test. Importantly, although for EVM beyond 11% rms, the *phase* regenerator does result in a decrease in phase noise, the *amplitude* regenerator decreases phase noise further. This is simply because of the conjugating effect of the amplitude regenerator which effectively allows the effects of SPM accrued during phase regeneration to be undone by the amplitude regenerator, as in [11].

Figure 4(f) clearly shows the benefits of performing amplitude regeneration after phase regeneration; phase regeneration actually results in an *increase* in EVM due to phase dependent gain and SPM, both of which are undone effectively by the amplitude regenerator. For an EVM_{in} of 7.3% rms, phase regeneration results in an increase in phase noise to $\mathrm{EVM}_{out} = 10.4\%$ rms whilst amplitude regeneration brings this back down to $\mathrm{EVM}_{out} = 7.3\%$ rms. The role of the amplitude regenerator is even more pronounced for the highest noise level tested with $\mathrm{EVM}_{in} = 17.7\%$ rms which increases to $\mathrm{EVM}_{in} = 18.3\%$ rms after phase regeneration but is brought back down to $\mathrm{EVM}_{in} = 9.8\%$ rms after amplitude regeneration. It could be argued that the phase regenerator is of little benefit here and that the amplitude regenerator is doing most of the work in improving the signal, however, this is not the case. If phase regeneration was not performed, the amplitude regenerator would provide no decrease in phase noise; the benefits of the PSA are simply masked by the increase in phase noise due to SPM that appears after this first stage alone.

Figures 4(g)– 4(i) show similar plots to those of Figs. 4(a)– 4(c), but with additional ASE, equivalent to the amount added in the highest noise case shown in plots Figs. 4(d)– 4(f). It can be seen that, even at this high noise level, the regenerator still manages to reduce both components of noise by a large margin. Figure 5(a) provides constellation plots for three input noise scenarios, at three different stages, before regeneration (orange), after phase regeneration alone (green) and after both phase and amplitude regeneration (blue). The constellation plots tell a similar story to the noise statistics. For the case where the signal has been contaminated with phase noise alone, (middle row Fig. 5(a)), phase regeneration reduces the phase noise of the signal whilst

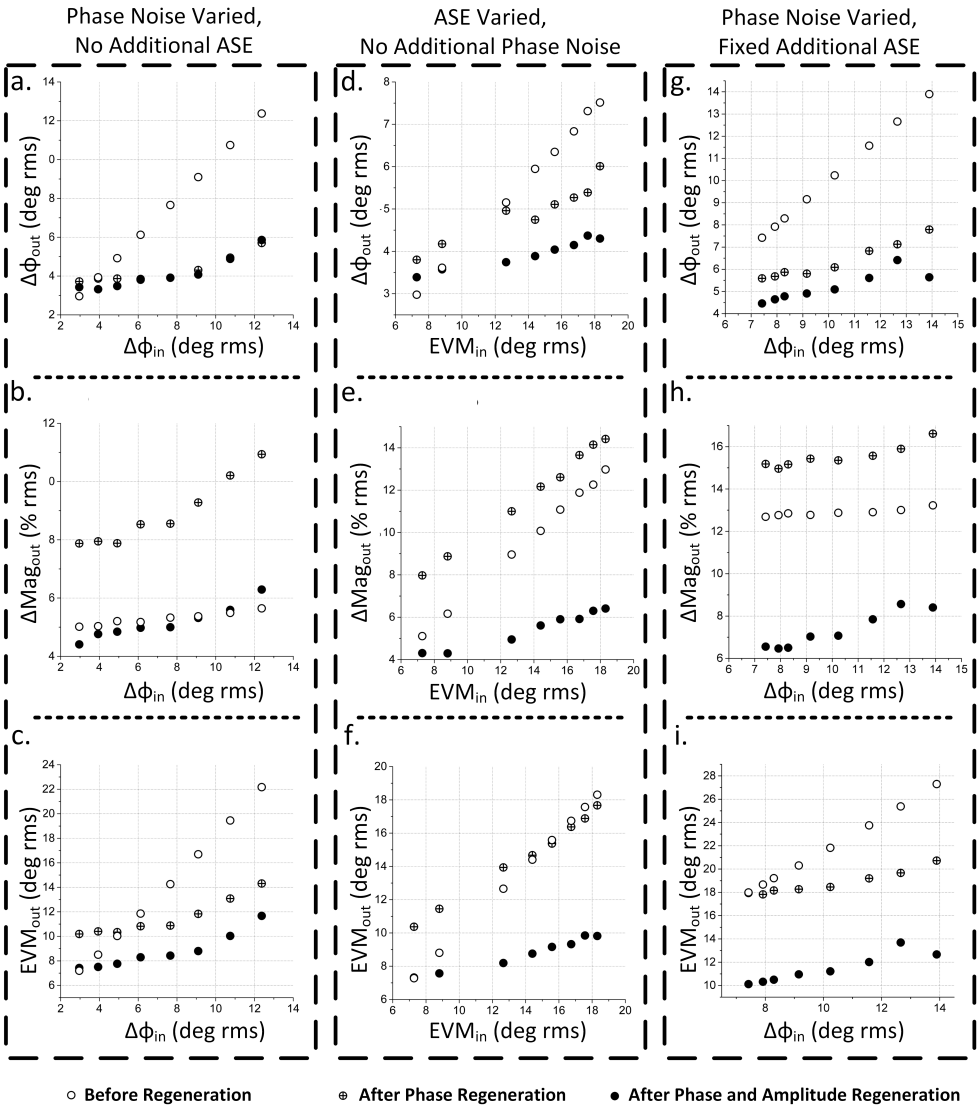

Fig. 4. $\Delta\phi$, ΔMag and EVM for three different noise scenarios.

increasing the amplitude noise due to the phase dependent gain of the system. This amplitude noise is undone effectively by the amplitude regenerator, resulting in a signal with a phase noise much reduced compared to the unregenerated input signal, and a comparable amplitude noise. For the highest noise scenario, which was obtained by contaminating the signal with both ASE and phase noise, we see that phase regeneration results in symbol clusters which, although having been squeezed radially, exhibit a characteristic SPM induced radial redistribution. Amplitude regeneration, once again, undoes this rotation as well as correcting for amplitude noise.

Finally, BER curves are presented both before any regeneration and after both phase and amplitude regeneration for the same noise levels in Fig. 5(b), the data being obtained using the OMA shown in Fig. 2, with the OSNR of the signal at the receiver controlled using the variable attenuator and EDFA identified in the receiver section of the set-up. With no additional

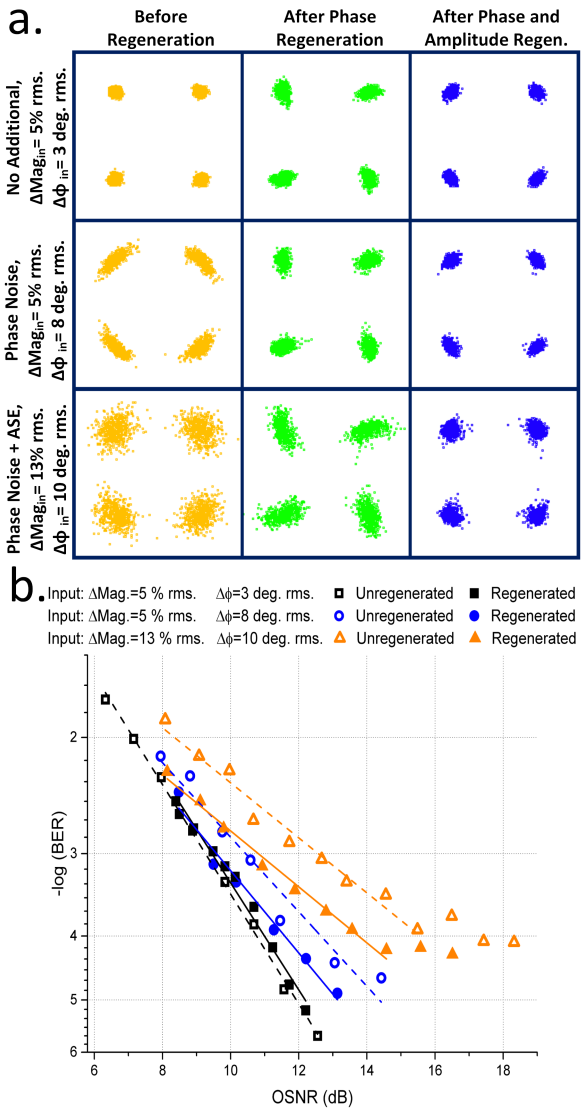

Fig. 5. (a) Constellation plots; (b) BER curves for the complete system with both sub-systems combined.

noise (plotted in black), regeneration can be seen to result in a very small power penalty of approximately 0.25 dB for all BERs. For the case where the signal was contaminated with phase noise alone, shown in blue, regeneration results in an improvement in receiver sensitivity of around 1.1 dB for all BERs. Finally, for the highest noise scenario, that corresponding to the addition of both ASE and phase noise, regeneration results in an improvement in receiver sensitivity of 1.8 dB, again, for all BERs except for those beyond 10^{-4} at which a noise floor is present due to the high amount of noise with which the input signal was contaminated.

5. Conclusion

The regeneration of both phase and amplitude of a noise loaded QPSK signal has been demonstrated by cascading a phase sensitive amplifier with a saturated FWM-based parametric amplifier. Given the conjugating nature of the amplitude limiter, it is possible to compensate for SPM accrued in the phase regenerating stage, permitting the use of higher operating powers of the phase regenerator which would otherwise have been prohibited due to the effects of SPM. The use of two cascaded regenerators allows each regenerator to be optimised for its specific role. Using the scheme, an effective halving of EVM for the highest noise case was demonstrated, with a corresponding improvement in receiver sensitivity of 1.8 dB for a BER of 10^{-4}.

Funding

Engineering and Physical Sciences Research Council (EP/I01196X).

Acknowledgments

This research is a part of the EPSRC Photonics Hyperhighway project. Dr F. Parmigiani is supported by a Royal Academy of Engineering/EPSRC research fellowship. The data for this work is accessible through the University of Southampton Institutional Research Repository (DOI:10.5258/SOTON/404345).